

# Passivation of Solution-Processed a-IGZO Thin-Film Transistor by Solution Processable Zinc Porphyrin Self-Assembled Monolayer

Maruti B. Zalte<sup>1</sup>, Tejas R. Naik<sup>1</sup>, A. Alka, M. Ravikanth, V. Ramgopal Rao<sup>2</sup>, *Fellow, IEEE*, and Maryam Shojaei Baghini<sup>1</sup>, *Senior Member, IEEE*

**Abstract**—Bottom-gate bottom contact amorphous indium gallium zinc oxide (a-IGZO) thin-film transistors (TFTs) were fabricated using solution processing. The nonpassivated a-IGZO-TFTs exhibited a significant threshold voltage shift, large hysteresis in the current–voltage characteristics, and degradation in the subthreshold swing. TFTs’ performance degradation is due to the interaction of its back channel with adsorbed oxygen and water molecules in the ambient air. The hydroxy-phenyl zinc porphyrin (ZnP) self-assembled monolayer (SAM) was formed on TFTs’ back channel using a low-cost solution-based approach to passivate TFTs back channel. The passivated a-IGZO-TFTs exhibited enhanced electrical characteristics and improved stability compared with nonpassivated TFTs. Passivated TFTs presented significantly reduced hysteresis up to 87% and subthreshold slope degradation up to 71%. The passivated TFTs showed excellent stability under positive (20 V) and negative (−20 V) bias stress conducted for 5000 s.

**Index Terms**—Amorphous indium gallium zinc oxide (a-IGZO), passivation, porphyrin, self-assembled monolayers (SAMs), solution process, thin-film transistor (TFT).

## I. INTRODUCTION

**S**OLUTION-PROCESSED amorphous indium gallium zinc oxide (a-IGZO) thin-film transistors (TFTs) have been extensively studied over conventional vacuum-processed TFTs for applications in flexible electronic displays, circuits, and sensors due to high carrier mobility and good uniformity with simple and low-cost fabrication process [1], [2]. A significant concern with a-IGZO-TFT is its performance in the ambient

atmosphere [3]. The adsorption of molecular species such as oxygen ( $O_2$ ) and water ( $H_2O$ ) on the indium gallium zinc oxide (IGZO) surface causes instability and a large hysteresis in the current–voltage characteristics of a-IGZO-TFTs [4], [5]. Furthermore, the solution-processed a-IGZO-TFTs are more sensitive to the ambient atmosphere because of the higher adsorption of gas molecules on a more coarsely packed a-IGZO layer [6]. Passivation of back channel of the a-IGZO-TFT is essential to improve its performance and stability in the ambient atmosphere. Inorganic-passivation layers such as  $SiO_2$  and  $SiN_x$  deposited using vacuum processes cause degradation of electrical characteristics of TFTs due to plasma-induced radiation damage to its back-channel region [7]. Furthermore, precise control of substrate temperature is crucial during deposition to ensure the passivation quality [8]. Solution-based passivation methods for a-IGZO-TFTs, using organic (CYTOP, SU8) and inorganic ( $Y_2O_3$ ) materials, are reported to overcome the issues associated with vacuum-processed inorganic passivation. The deionized (DI) water-based yttrium oxide ( $Y_2O_3$ ) passivation showed a significant improvement in the performance and stability of TFTs; however, the process involved spin coating (3000 r/min, 30 s) and annealing at 250 °C for 5 h in vacuum [9]. The SU-8 resist as a passivation layer of a-IGZO-TFTs showed improvement in the device performance where the process involved spin coating and annealing at 200 °C for 1 h [10]. The organic CYTOP-passivation layer for a-IGZO-TFT formed by spin coating exhibited good electrical characteristic where the annealing temperature was 180 °C for 1 h [11]. These reported solution-processed passivation methods involve spin coating and annealing temperatures more than 180 °C. Back-channel passivation of a-IGZO-TFTs with self-assembled monolayers (SAMs) offers several advantages [12]–[14]. The proposed zinc porphyrin (ZnP)-SAM passivation avoids the plasma damage of IGZO surface, forms chemically stable interface with IGZO surface, and is important for passivation of traps (−OH) in the back channel. The low-cost processing and room-temperature formation of SAMs are some of the other benefits compared with the existing passivation methods.

In this work, we report hydroxy-phenyl ZnP-SAM for back-channel passivation of the solution-processed a-IGZO-TFT. It involves a simple passivation scheme that can eas-

Manuscript received July 4, 2021; revised August 10, 2021 and August 30, 2021; accepted September 6, 2021. Date of publication September 22, 2021; date of current version October 22, 2021. This work was supported by the Department of Science and Technology (DST), Government of India under Grant SR/NM/TP-56/2016-IITB (G). The review of this brief was arranged by Editor H. Klauk. (*Corresponding author: Maruti B. Zalte.*)

Maruti B. Zalte, Tejas R. Naik, V. Ramgopal Rao, and Maryam Shojaei Baghini are with the Department of Electrical Engineering, IIT Bombay, Mumbai 400076, India (e-mail: marutizalte@iitb.ac.in; trnaik@ee.iitb.ac.in; rrao@ee.iitb.ac.in; mshojaei@ee.iitb.ac.in).

A. Alka and M. Ravikanth are with the Department of Chemistry, IIT Bombay, Mumbai 400076, India (e-mail: alchinnu@gmail.com; ravikanth@chem.iitb.ac.in).

Color versions of one or more figures in this article are available at <https://doi.org/10.1109/TED.2021.3111542>.

Digital Object Identifier 10.1109/TED.2021.3111542

ily be integrated with the solution-processed a-IGZO-TFT fabrication. SAM facilitated a barrier layer for the adsorption of  $O_2/H_2O$  molecules, passivated traps on TFTs' back channel, and contributed to performance enhancement and stability. Modification in the chemical properties of a-IGZO-TFTs' back channel after ZnP-SAM layer formation and its impact on devices' electrical performance and stability are investigated systematically.

## II. EXPERIMENTAL PROCEDURE

The 0.1-M IGZO solution was synthesized as per process mentioned by Rim *et al.* [15]. 5N purity metal precursors [225.6 mg of indium nitrate hydrate ( $In(NO_3)_3 \cdot xH_2O$ ; molar mass = 300.83 g/mol), 21.3 mg of gallium nitrate hydrate ( $Ga(NO_3)_3 \cdot xH_2O$ ; molar mass = 255.74 g/mol), and 31.5-mg zinc nitrate hydrate ( $Zn(NO_3)_2 \cdot xH_2O$ ; molar mass = 189.40 g/mol) dissolved in 10-mL 2-methoxyethanol. Additives, namely 100- $\mu$ L acetylacetonone (aq) and 40- $\mu$ L ammonium hydroxide (aq) (28.0%  $NH_3$  in water), added to the mixer to enhance the oxidation process [15]. Bottom-gate bottom contact TFTs were fabricated on silicon substrates. The substrate consisted of an n-doped ( $n \approx 3 \times 10^{17} \text{ cm}^{-3}$ ) silicon (100) which also acts as a gate, the thermally grown 100-nm  $SiO_2$  as the gate dielectric, and the interdigitated source/drain terminals (indium tin oxide (ITO)-gold) patterned on  $SiO_2$  to ensure larger width to length ratio ( $W/L = 10\ 000 \mu\text{m}/20 \mu\text{m}$ ). The substrates were ultrasonically cleaned in acetone and isopropyl alcohol for 10 min each and dehydrated at 120  $^\circ\text{C}$  for 5 min to remove water traces. Furthermore, UV ozone cleaning was done for 10 min to remove organic contaminants and improve the surface's wetting. The cleaned substrates were immediately spin-coated with the synthesized IGZO solution at 3000 r/min for 30 s and annealed at 300  $^\circ\text{C}$  for 3 h in the ambient air. The passivation process involved preparation of ZnP solution and the formation of SAM on the fabricated a-IGZO-TFT surface. The  $10^{-4}$  M ZnP solution was prepared by dissolving ZnP in toluene. Furthermore, fabricated TFTs were placed in ZnP solution for 1 h in airtight condition. The details of ZnP and its molecular preparation are given elsewhere [16], [17]. The SAM was bonded to the hydroxyl molecules present on IGZO surface via the OH functionalization due to strong intermolecular forces (hydrogen bond) [17]. The samples were then dried using dry nitrogen flow and annealed at 100  $^\circ\text{C}$  for 10–20 min. The schematic of a-IGZO-TFT structure modified with ZnP-SAM layer is shown in Fig. 1. The thickness of the a-IGZO and ZnP-SAM layer, measured using a cross-sectional field emission scanning electron microscope (FE-SEM), was  $\approx 8$  and  $\approx 2$  nm, respectively, which is consistent with previous studies [16], [17] and is confirmed by X-ray photoelectron spectroscopy (XPS) depth profile. All characterizations were performed on TFTs before and after SAM passivation to study the impact of passivation on device performance and the stability in ambient air.

## III. RESULTS AND DISCUSSION

### A. UV-Visible Spectroscopy

The UV-Vis measurement of the a-IGZO surface before and after SAM formation was performed. As seen from Fig. 2, a

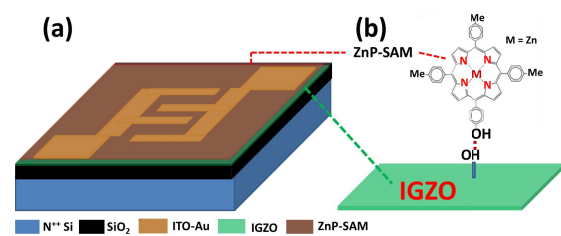


Fig. 1. (a) a-IGZO-TFT structure with ZnP-SAM layer on the back channel. (b) ZnP-SAM structure and SAM formation on IGZO surface.

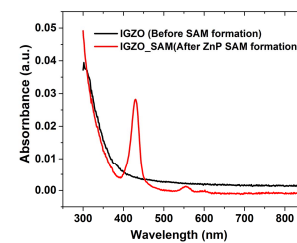


Fig. 2. UV-vis spectra of a-IGZO before and after ZnP-SAM formation.

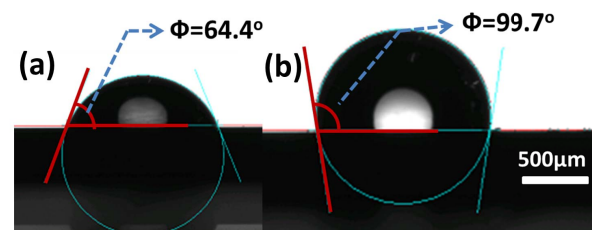


Fig. 3. Contact angle (a) a-IGZO before and (b) a-IGZO after, SAM formation.

distinct peak at 430 nm confirms the ZnP-SAM formation on the a-IGZO surface. The UV-Vis result is consistent with the reported literature [16].

### B. Contact Angle Measurement

Contact angle measurements were carried out to acquire information about the a-IGZO surface coverage after ZnP-SAM formation (Fig. 3). The increased contact angle suggests the surface modification from hydrophilic to hydrophobic due to the hydrophobic nature of the methyl ( $-CH_3$ ) groups in SAM molecules [17]. Furthermore, the excellent surface coverage of ZnP-SAM on the back channel of TFT reduces adsorption of  $O_2/H_2O$ , enhancing its performance in the ambient air.

### C. Atomic Force Microscopy

Atomic force microscopy (AFM) analysis (Fig. 4) was carried out to study the surface modification of a-IGZO after SAM formation. The root mean square (rms) roughness of a-IGZO before and after the ZnP-SAM layer was 1.17 and 1.48 nm, respectively. The roughness of the a-IGZO surface did not change considerably after SAM formation, indicating homogeneous surface coverage of the SAM layer on the a-IGZO surface with little or no multilayer formation which is consistent with the reported literature [12], [17].

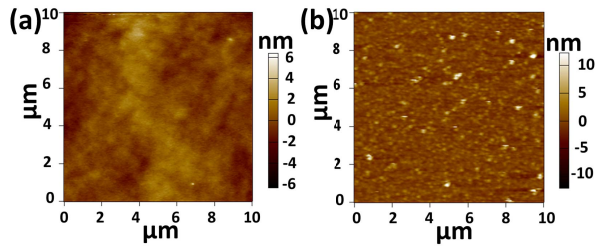


Fig. 4. AFM topography images of (a) a-IGZO before and (b) a-IGZO after, ZnP-SAM monolayer formation (images scale:  $10 \mu\text{m} \times 10 \mu\text{m}$ ).

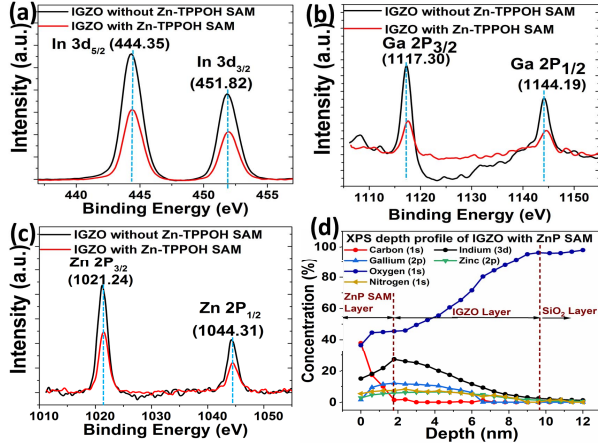


Fig. 5. XPS spectra. (a) Indium, (b) gallium, and (c) zinc of a-IGZO film before and after ZnP-SAM formation. (d) XPS depth profile of a-IGZO film after ZnP-SAM formation.

#### D. X-Ray Photoelectron Spectroscopy

XPS measurements were performed to investigate the favorable effect of surface modification by SAM molecules and binding modes of SAM to the a-IGZO surface. XPS peaks for In, Ga, and Zn are matching with the standard peaks [at binding energies for their chemical states  $\text{In}_2\text{O}_3$  ( $\text{In}_{3d_{5/2}}$ ),  $\text{Ga}_2\text{O}_3$  ( $\text{Ga}_{2P_{3/2}}$ ), and  $\text{ZnO}$  ( $\text{Zn}_{2P_{3/2}}$ )] at 444, 1117, and 1021 eV, respectively, depicted in Fig. 5(a)–(c). The peak positions were unchanged after SAM formation, suggesting no SAM bonding with In, Ga, and Zn [17]. The reduction in peak intensities after SAM formation can be attributed to the attenuation of photoelectrons originating from the bulk a-IGZO film [12]. The XPS depth profile was performed to check the bonding changes in the bulk IGZO film underneath the ZnP-SAM. As seen in Fig. 5(d), the concentration of carbon is highest at the top of SAM functionalized IGZO surface, gradually becoming zero at a depth of 2 nm, ensuring no bonding changes in the IGZO bulk. The concentration of In, Ga, and Zn is highest in the bulk IGZO (2–8 nm) and it gradually decreases for the depth near the IGZO/ $\text{SiO}_2$  interface. The SAM bonded to hydroxyl molecules present on the a-IGZO surface [12], confirmed by the changed shape of O1s peaks, as seen in Fig. 6. The deconvoluted O1s Gaussian distributed peaks centered at  $529.59 \text{ eV} \pm 0.07 \text{ eV}$ ,  $530.63 \text{ eV} \pm 0.1 \text{ eV}$ , and  $531.62 \text{ eV} \pm 0.03 \text{ eV}$  (with the full-width at half-maximum (FWHM)  $\approx 1.62 \text{ eV} \pm 0.1 \text{ eV}$  for all peaks) are attributed to the  $\text{O}_2$  ions bonding with metal ions ( $\text{O}_M$ ), oxygen

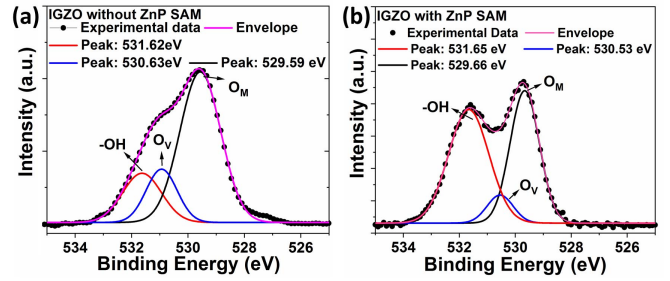


Fig. 6. XPS O1s spectra. (a) a-IGZO before and (b) a-IGZO after ZnP-SAM formation.

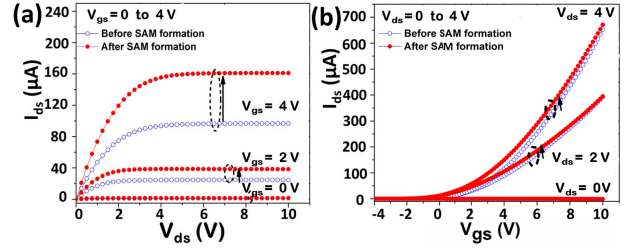


Fig. 7. (a)  $I_{ds}$ – $V_{ds}$  and (b)  $I_{ds}$ – $V_{gs}$  characteristic before and after SAM formation.

TABLE I  
IGZO-TFTs' PARAMETERS BEFORE AND AFTER ZNP-SAM PASSIVATION

Parameter	a-IGZO-TFTs Before passivation	a-IGZO-TFTs After passivation
$V_{TH}$ (V)	$0.9 \pm 0.2$	$0.2 \pm 0.05$
SS (V/dec)	$0.8 \pm 0.2$	$0.4 \pm 0.1$
$\mu$ ( $\text{cm}^2/\text{V}\cdot\text{s}$ )	$3.5 \pm 0.5$	$8.5 \pm 0.5$
$V_{HYS}$ (V)	$1.2 \pm 0.2$	$0.3 \pm 0.1$

vacancy ( $\text{O}_V$ ), and weakly bound oxygen species ( $-\text{CO}_3$ ,  $-\text{OH}$ , and adsorbed  $\text{O}_2$ ) on the surface in stoichiometric IGZO surface. The increased OH peaks of the a-IGZO surface after ZnP-SAM passivation are attributed to the binding of SAM molecules on the IGZO surface. The decrease in the  $\text{O}_M$  and  $\text{O}_V$  peaks can be assigned to the formation monolayers that results in reduction of photoelectrons originated from the bulk IGZO.

#### E. Electrical Characterization

The current–voltage ( $I$ – $V$ ) characteristics of TFTs before (nonpassivated) and after ZnP-SAM (passivated) layer formation were measured in the ambient air (relative humidity  $50\% \pm 3\%$  and temperature  $24^\circ\text{C}$ ). As depicted in the output ( $I_{ds}$ – $V_{ds}$ ) characteristics [Fig. 7(a)], there was a significant increase in drain current of the SAM passivated TFT. The transfer ( $I_{ds}$ – $V_{gs}$ ) characteristics [Fig. 7(b)] showed negative shift of threshold of a TFT after SAM passivation.

The threshold voltage ( $V_{TH}$ ), subthreshold slope (SS), mobility ( $\mu$ ), and hysteresis voltage ( $V_{HYS}$ ) were extracted from  $I$ – $V$  to study the performance enhancement of TFTs

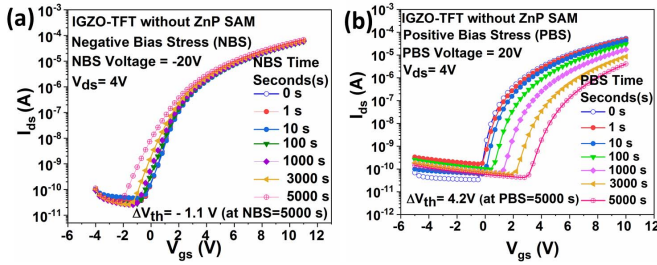


**Fig. 8.**  $I_{ds}$ - $V_{gs}$  characteristics of nonpassivated a-IGZO-TFT. (a) Negative bias ( $-20$  V) and (b) positive bias ( $20$  V), stress for 1–5000 s.

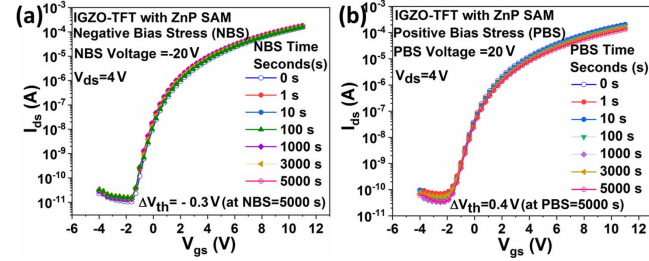


**Fig. 9.**  $I_{ds}$ - $V_{gs}$  characteristics of ZnP-SAM passivated a-IGZO-TFT. (a) Negative bias ( $-20$  V) and (b) positive bias ( $20$  V), stress for 1–5000 s.

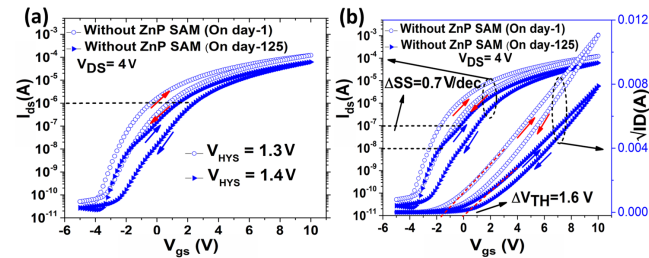


**Fig. 10.**  $I_{ds}$ - $V_{gs}$  characteristics of nonpassivated a-IGZO-TFT on day 1 and day 125 after fabrication. (a)  $V_{HYS}$ . (b) Impact on  $V_{TH}$  and SS.

after ZnP-SAM passivation. The average values of extracted parameters and their deviation of multiple TFTs before and after passivation are summarized in Table I. The performance enhancement of TFTs can be attributed to reductions of adsorbed species ( $O_2/H_2O$ ) and passivation of charge traps (OH) in the back channel [13]. Furthermore, to investigate the impact of passivation on stability of TFTs, the bias stress tests, the long-term stability in ambient air, and DI water dip tests were performed. The negative bias stress (NBS;  $V_{gs} = -20$  V) and positive bias stress (PBS;  $V_{gs} = 20$  V) for 1–5000 s were performed on TFTs in the ambient air to confirm passivation layer's effectiveness [18]. As depicted in Fig. 8(a), a considerable negative  $V_{TH}$  shift ( $\Delta V_{TH} = -1.0$  V  $\pm$  0.2 V) and SS degradations observed in the nonpassivated TFTs exposed to NBS. The PBS resulted in significant positive  $V_{TH}$  shift ( $\Delta V_{TH} = 4.0$  V  $\pm$  0.5 V) and SS degradations, as seen in Fig. 8(b). The passivated TFTs exposed to NBS [Fig. 9(a)] and PBS [Fig. 9(b)] showed a significant improvement in the  $I$ - $V$  characteristics. A minor  $V_{TH}$  shift during NBS ( $\Delta V_{TH} = -0.25$  V  $\pm$  0.05 V) and PBS ( $\Delta V_{TH} = 0.35$  V  $\pm$  0.05 V) and significantly reduced

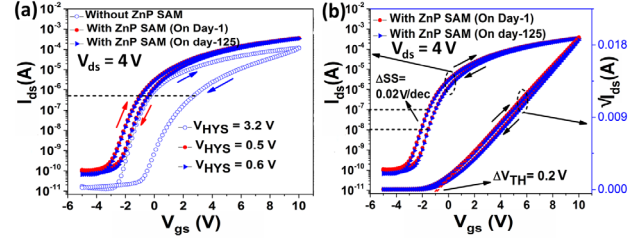


**Fig. 11.**  $I_{ds}$ - $V_{gs}$  characteristics a-IGZO-TFT on day 1 and day 125. (a)  $V_{HYS}$  of nonpassivated and ZnP-SAM passivated a-IGZO-TFT. (b) Impact on  $V_{TH}$  and SS in ZnP-SAM passivated a-IGZO-TFT.

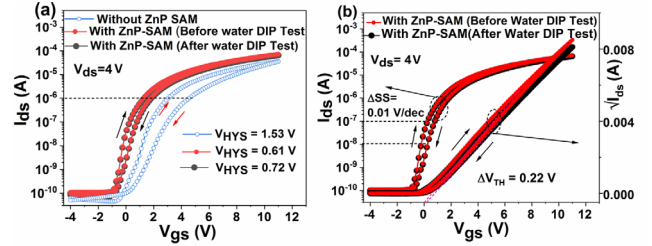


**Fig. 12.**  $I_{ds}$ - $V_{gs}$  characteristics of ZnP-SAM passivated a-IGZO-TFT before and after DI water dip test. (a)  $V_{HYS}$ . (b) Impact on  $V_{TH}$  and SS.

**TABLE II**  
STABILITY OF ZNP-SAM PASSIVATED IGZO-TFTS

Test	Parameter	Non-Passivated	SAM- Passivated
		IGZO-TFTs	IGZO-TFTs
Long-term	$\Delta V_{HYS}$ (V)	$1.0 \pm 0.2$	$0.1 \pm 0.05$
Stability	$\Delta V_{TH}$ (V)	$1.4 \pm 0.2$	$0.2 \pm 0.1$
	$\Delta SS$ (V/dec)	$0.7 \pm 0.3$	$0.02 \pm 0.005$
DI-water	$\Delta V_{HYS}$ (V)	$1.6 \pm 0.1$	$0.4 \pm 0.1$
dip test	$\Delta V_{TH}$ (V)	$1.3 \pm 0.1$	$0.2 \pm 0.05$
	$\Delta SS$ (V/dec)	$0.8 \pm 0.3$	$0.01 \pm 0.008$

SS degradation were observed compared with nonpassivated TFTs. The long-term stability (125 days after fabrication) of nonpassivated and passivated TFTs stored in ambient air was investigated. As seen from Fig. 10(a), the nonpassivated TFTs showed significant clockwise hysteresis, which further increased after 125 days. The degradation in SS and a considerable shift in  $V_{TH}$  were observed, as seen from Fig. 10(b). The performance degradation in nonpassivated TFTs can be attributed to the charge transfer by adsorbed  $O_2/H_2O$  molecules on the TFTs' back channel. Adsorbed  $O_2$  depletes the electron carriers on a-IGZO film, and  $H_2O$  induces the formation of an accumulation layer of extra electron carriers. The adsorbed  $H_2O$  also acts as acceptor-like trap sites [4], [19], which trap electrons during the forward sweep of gate bias resulting in a partial depletion of the channel. Hence, during the gate bias's reverse sweep, transfer characteristics are shifted toward higher voltages [8]. The SAM layer formed on the back channel serves as an effective barrier for  $O_2$  and  $H_2O$  molecules. SAM also passivates traps ( $-OH$ ) by reacting with them [13]. The reduction of adsorbed species and charge traps on the back channel resulted in TFTs with enhanced performance and stability in the ambient air. After passivation,

$V_{HYS}$  reduced up to 87%, and SS degradation was reduced up to 71%, as depicted in Fig. 11(a) and (b), respectively. The  $I-V$  of ZnP-passivated a-IGZO-TFTs was nearly identical after 125 days. To investigate the effect of H<sub>2</sub>O molecules on performance after passivation, TFTs were dipped in DI water for 1 min, later dried by the flow of dry nitrogen (DI water dip test) [13]. The  $I-V$  of passivated TFTs were found nearly identical after the DI water dip test (Fig. 12). The results of the stability tests performed before and after ZnP-SAM passivation are summarized in Table II. The average shift in parameter value and its deviation for multiple TFTs used in the study are indicated.

A significant improvement in the stability was observed in the ZnP-SAM passivated a-IGZO-TFTs.

#### IV. CONCLUSION

IGZO-TFTs' performance enhancement fabricated using low-cost solution processes with the back channel passivated by ZnP-SAM is demonstrated. The a-IGZO-TFT after ZnP-SAM passivation exhibited improved electrical performance and stability due to the reduction in adsorption of water and oxygen molecules on its back channel. The passivated TFTs' performance was unchanged after prolonged exposure (125 days) to the ambient air and after the dipping TFTs in DI water for 1 min. The passivated TFTs showed a minor shift of threshold voltage, up to 87% reduction in the hysteresis voltage, and 71% reduction in SS. The passivated TFTs showed excellent stability when exposed to positive and negative bias stress. Solution processing and back-channel passivation using solution-phase ZnP-SAMs can be a cost-effective approach to fabricate electrically stable a-IGZO-TFTs.

#### ACKNOWLEDGMENT

The authors would like to thank Center for Excellence in Nanoelectronics (CEN), Indian Institute of Technology Bombay Nanofabrication Facility (IITBNF)-IIT-Bombay nanofabrication facility for device fabrication and characterization.

#### REFERENCES

- [1] S. J. Kim, S. Yoon, and H. J. Kim, "Review of solution-processed oxide thin-film transistors," *Jpn. J. Appl. Phys.*, vol. 53, no. 2S, Feb. 2014, Art. no. 02BA02.
- [2] K. Nomura, H. Ohta, A. Takagi, T. Kamiya, M. Hirano, and H. Hosono, "Room temperature fabrication of transparent flexible thin film transistors using amorphous oxide semiconductors," *Nature*, vol. 432, pp. 488–492, Nov. 2004.
- [3] J. Park, J. Jeong, H. Chung, Y. Mo, and H. Kim, "Electronic transport properties of amorphous indium gallium zinc oxide upon exposure to water," *Appl. Phys. Lett.*, vol. 92, Feb. 2008, Art. no. 072104, doi: 10.1063/1.2838380.
- [4] D. Kim, S. Yoon, Y. Jeong, Y. Kim, and M. Hong, "Role of adsorbed H<sub>2</sub>O on transfer characteristics of solution-processed zinc tin oxide thin-film transistors," *Appl. Phys. Exp.*, vol. 5, Jan. 2012, Art. no. 021101, doi: 10.1143/APEX.5.021101.
- [5] W.-T. Chen *et al.*, "Oxygen-dependent instability and annealing/passivation effects in amorphous In-Ga-Zn-O thin-film transistors," *IEEE Electron Device Lett.*, vol. 32, no. 11, pp. 1552–1554, Nov. 2011, doi: 10.1109/LED.2011.2165694.
- [6] S. Lee and J. Jeong, "Electrical stability of solution-processed a-IGZO TFTs exposed to high-humidity ambient over long periods," *IEEE J. Electron Device Soc.*, vol. 7, pp. 26–32, Oct. 2018, doi: 10.1109/JEDS.2018.2875755.
- [7] S. Kim *et al.*, "New approach for passivation of Ga<sub>2</sub>O<sub>3</sub>-In<sub>2</sub>O<sub>3</sub>-ZnO thin film transistors," in *IEDM Tech. Dig.*, Dec. 2007, pp. 583–586.
- [8] S. Choi and M. Han, "Effect of deposition temperature of SiO<sub>x</sub> Passivation layer on the electrical performance of a-IGZO TFTs," *IEEE Electron Device Lett.*, vol. 33, no. 3, pp. 396–398, Mar. 2012, doi: 10.1109/LED.2011.2181320.
- [9] R. N. Bukke, C. Avis, and J. Jang, "Solution-processed amorphous In-Zn-Sn oxide thin-film transistor performance improvement by solution-processed Y<sub>2</sub>O<sub>3</sub> passivation," *IEEE Electron Device Lett.*, vol. 37, no. 4, pp. 433–436, Apr. 2016, doi: 10.1109/LED.2016.2528288.
- [10] A. Olziersky *et al.*, "Insight on the SU-8 resist as passivation layer for transparent Ga<sub>2</sub>O<sub>3</sub>-In<sub>2</sub>O<sub>3</sub>-ZnO thin-film transistors," *J. App. Phys.*, vol. 108, no. 6, Sep. 2010, Art. no. 064505, doi: 10.1063/1.3477192.
- [11] S.-H. Choi, J.-H. Jang, J.-J. Kim, and M.-K. Han, "Low-temperature organic (CYTOP) passivation for improvement of electric characteristics and reliability in IGZO TFTs," *IEEE Electron Device Lett.*, vol. 33, no. 3, pp. 381–383, Mar. 2012, doi: 10.1109/LED.2011.2178112.
- [12] W. Xu, D. Liu, H. Wang, L. Ye, Q. Miao, and J.-B. Xu, "Facile passivation of solution-processed InZnO thin-film transistors by octadecylphosphonic acid self-assembled monolayers at room temperature," *Appl. Phys. Lett.*, vol. 104, Feb. 2014, Art. no. 051607.
- [13] P. Xiao *et al.*, "InGaZnO thin-film transistors modified by self-assembled monolayer with different alkyl chain length," *IEEE Electron Device Lett.*, vol. 104, no. 7, May 2014, Art. no. 173504, doi: 10.1109/LED.2015.2431741.
- [14] X. Du, B. T. Flynn, J. R. Motley, W. F. Stickle, H. Bluhm, and G. S. Herman, "Role of self-assembled monolayers on improved electrical stability of amorphous In-Ga-Zn-O thin-film transistors," *ECS J. Solid State Sci. Technol.*, vol. 3, no. 9, pp. Q3045–Q3049, 2014, doi: 10.1149/2.010409jss.
- [15] Y. Rim, H. Chen, Y. Liu, S. Bae, H. Kim, and Y. Yang, "Direct light pattern integration of low-temperature solution-processed all-oxide flexible electronics," *ACS Nano*, vol. 8, no. 9, pp. 9680–9686, 2014.
- [16] T. Naik, V. Singh, M. Ravikanth, and V. Rao, "A vapor phase self-assembly of porphyrin monolayer as copper diffusion barrier for back-end-of-line CMOS technology," *IEEE Trans. Electron Devices*, vol. 63, no. 5, pp. 2009–2015, May 2016, doi: 10.1109/TED.2016.2537370.
- [17] M. Garg, T. Naik, C. Pathak, S. Natarajan, V. Rao, and R. Singh, "Significant improvement in the electrical characteristics of Schottky barrier diodes on molecularly modified gallium nitride surfaces," *Appl. Phys. Lett.*, vol. 112, no. 16, Apr. 2018, Art. no. 163502, doi: 10.1063/1.5005587.
- [18] S. Hong, S. P. Park, Y.-G. Kim, B. H. Kang, J. W. Na, and H. J. Kim, "Low-temperature fabrication of an HfO<sub>2</sub> passivation layer for amorphous indium-gallium-zinc oxide thin film transistors using a solution process," *Sci. Rep.*, vol. 7, no. 1, pp. 1–9, Nov. 2017, doi: 10.1038/s41598-017-16585-x.
- [19] W. Hung *et al.*, "Influence of H<sub>2</sub>O dipole on subthreshold swing of amorphous indium-gallium-zinc-oxide thin film transistors," *Electrochem. Solid-State Lett.*, vol. 14, p. H114, Dec. 2010, doi: 10.1149/1.3526097.